Biochimica et Biophysica Acta 1808 (2011) 2753–2760

Contents lists available at ScienceDirect

Biochimica et Biophysica Acta

journal homepage: www.elsevier.com/locate/bbamem

Effect of ceramide structure on membrane biophysical properties: The role of acyl chain length and unsaturation

Sandra N. Pinto [a], Liana C. Silva [b,*], Anthony H. Futerman [c], Manuel Prieto [a]

[a] Centro de Química-Física Molecular and Institute of Nanoscience and Nanotechnology, Instituto Superior Técnico, U.T.L, Complexo I, Av. Rovisco Pais, 1049–001 Lisboa, Portugal
[b] iMed.UL-Research Institute for Medicines and Pharmaceutical Sciences, Faculdade de Farmácia, Universidade de Lisboa, Av. Prof. Gama Pinto, 1649–003 Lisboa, Portugal
[c] Department of Biological Chemistry, Weizmann Institute of Sciences, Rehovot 76100, Israel

ARTICLE INFO

Article history:
Received 6 June 2011
Received in revised form 13 July 2011
Accepted 15 July 2011
Available online 30 July 2011

Keywords:
Ceramide gel domains
Ceramide synthases
Ceramide tubules
Interdigitation
Lipid domain morphology

ABSTRACT

Ceramide is an important bioactive sphingolipid involved in a variety of biological processes. The mechanisms by which ceramide regulates biological events are not fully understood, but may involve alterations in the biophysical properties of membranes. We now examine the properties of ceramide with different acyl chains including long chain (C16- and C18-), very long chain (C24-) and unsaturated (C18:1- and C24:1-) ceramides, in phosphatidylcholine model membranes. Our results show that i) saturated ceramides have a stronger impact on the fluid membrane, increasing its order and promoting gel/fluid phase separation, while their unsaturated counterparts have a lower (C24:1-) or no (C18:1-) ability to form gel domains at 37 °C; ii) differences between saturated species are smaller and are mainly related to the morphology and size of the gel domains, and iii) very long chain ceramides form tubular structures likely due to their ability to form interdigitated phases. These results suggest that generation of different ceramide species in cell membranes has a distinct biophysical impact with acyl chain saturation dictating membrane lateral organization, and chain asymmetry governing interdigitation and membrane morphology.

1. Introduction

Sphingolipids (SLs) are important components of biological membranes and are involved in a variety of biological functions ranging from cell proliferation to apoptosis [1–3]. Ceramide is one of most important bioactive SLs, and comprises a fatty acid (which can be either saturated or monounsaturated) of variable chain length (C14–C26) linked by an amide bond to C2- of the long chain base, sphingosine (Fig. 1) [4]. In mammals, de *novo* ceramide synthesis is regulated by a family of six ceramide synthases (CerS) that have different specificities towards fatty acyl CoAs with various acyl chain lengths. Thus, CerS1 and CerS5 use long acyl chain CoAs (C18- and C16-, respectively), while CerS2 and CerS3 are involved in the synthesis of very long acyl chain ceramides (>C22) [5]. Ceramide can also be generated in the plasma membrane through the hydrolysis of sphingomyelin (SM). Both pathways can be activated in response to stress stimuli [6], driving an increase in cellular ceramide and consequent activation of cellular processes, including apoptotic signaling pathways [2].

It has been postulated that the distinct biophysical properties of ceramide play a major role in the regulation of ceramide-dependent signaling pathways [2]. Moreover, ceramides with different acyl-chains appear to have distinct physiological actions, which may be due to their different impact on the biophysical properties of membranes. As an example, mixing ceramide with fluid lipids [7–9], or generating ceramide through SM hydrolysis [10–13] in model membranes, drives an increase in the order of the membrane [14], induces gel-fluid phase separation [9,14,15], promotes the formation of non-lamellar structures [9] and/or induces morphological alterations of the vesicles [16]. Although some studies have explored the effect of different ceramides on the biophysical properties of model membranes [7,9,17], information is still lacking regarding the differential impact of long chain versus very long chain ceramides and the role of unsaturated chains compared to saturated chains. To date, most biophysical studies have focused on the chain length [7,18], the role of chain asymmetry [19,20] or on the properties of the non-physiological short chain (i.e. C2-6) ceramides [9]. In addition, some of these studies were performed using ceramide from natural sources which contain a mixture of different

Abbreviations: C16-ceramide, N-palmitoyl-D-*erythro*-sphingosine; C18:1-ceramide, N-oleoyl-D-*erythro*-sphingosine; C18-ceramide, N-stearoyl-D-*erythro*-sphingosine; C24:1-ceramide, N-nervonoyl-D-*erythro*-sphingosine; C24-ceramide, N-lignoceroyl-D-*erythro*-sphingosine; CerS, ceramide synthases; DPH, 1,6-diphenyl-1,3,5-hexatriene; FCS, Fluorescence correlation spectroscopy; GUV, giant unilamellar vesicles; MLV, multilamellar vesicles; POPC, 1-palmitoyl-2-oleoyl-*sn*-glycero-3-phosphocholine; Rho 110, rhodamine 110; Rho-DOPE, N-rhodamine-dipalmitoylphosphatidylethanolamine; SLs, Sphingolipids; SM, sphingomyelin; t-PnA, trans-parinaric acid

* Corresponding author. Tel.: +351 217 946 400x14245; fax: +351 217 937 703.
E-mail address: lianacsilva@ff.ul.pt (L.C. Silva).

0005-2736/$ – see front matter © 2011 Elsevier B.V. All rights reserved.
doi:10.1016/j.bbamem.2011.07.023

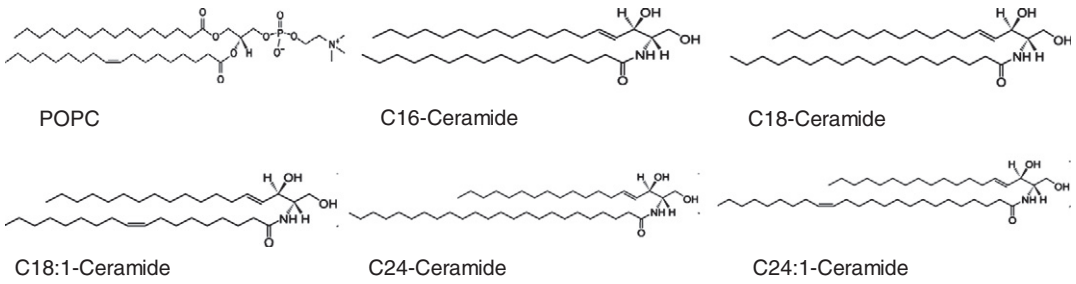

Fig. 1. Structures of the lipids used in this study.

acyl chain lengths. These are possible reasons for some of the discrepancies between different studies [20–22].

To address the impact of ceramide acyl chain structure, it is important to systematically analyze the effects of varying the acyl chain length and the degree of unsaturation. We now show that i) saturated ceramides have a stronger tendency to increase the order of the fluid membranes and to segregate into highly ordered gel domains compared to their unsaturated counterparts; ii) the impact of saturated ceramides in the properties of the fluid membrane is similar, changing only to a small extent with acyl chain length. However, the size and morphology of the domains formed by each saturated ceramide is significantly different; iii) very long chain ceramides are able to promote the formation of interdigitated phases and induce strong morphological alterations, such as tubules, independently of the degree of unsaturation; iv) the long chain unsaturated ceramide is unable to increase the order of the membrane or promote gel-fluid phase separation at physiological temperatures. Therefore, it is expected that generation of distinct ceramides in cell membranes would have a different biophysical impact with acyl chain saturation dictating membrane lateral organization and chain asymmetry governing interdigitation and membrane morphology. The global biophysical effect of increasing ceramide levels might therefore depend on the balance between long chain versus very long chain, and saturated versus unsaturated ceramide species.

2. Materials and methods

2.1. Materials

POPC, C16-, C18-, C18:1-, C24-, C24:1-ceramide (1-palmitoyl-2-oleoyl-*sn*-glycero-3-phosphocholine, N-palmitoyl-D-*erythro*-sphingosine, N-stearoyl-D-*erythro*-sphingosine, N-oleoyl-D-*erythro*-sphingosine, N-lignoceroyl-D-*erythro*-sphingosine; N-nervonoyl-D-*erythro*-sphingosine) and Rho-DOPE (N-rhodamine-dipalmitoylphosphatidylethanolamine) (Fig. 1) were obtained from Avanti Polar Lipids (Alabaster, AL). DPH (1,6-diphenyl-1,3,5-hexatriene), t-PnA (trans-parinaric acid), and Rho 110 (rhodamine 110) were from Molecular Probes (Leiden, The Netherlands). All organic solvents were UVASOL grade from Merck (Darmstadt, Germany).

2.2. Fluorescence spectroscopy

To evaluate the effect of ceramide structure on membrane properties, multilamellar vesicles (MLV) (total lipid concentration of 0.1 mM) were prepared as described [8]. The suspension medium was 10 mM sodium phosphate, 150 mM NaCl, 0.1 mM EDTA buffer (pH 7.4). Fluorescence anisotropy of t-PnA or DPH (at a probe/lipid ratio of 1/500 and 1/250, respectively) was measured in a SLM Aminco 8100 series 2 spectrofluorimeter with double excitation and emission monochromators, MC400 (Rochester, NY). All measurements were performed in 0.5 cm × 0.5 cm quartz cuvettes under magnetic stirring. The excitation (λ_{exc})/emission (λ_{em}) wavelengths were 305/405 nm for t-PnA and 358/430 nm for DPH. Constant temperature was maintained using a Julabo F25 circulating water bath controlled with 0.1 °C precision directly inside the cuvette with a type-K thermocouple (Electrical Electronic Corp., Taipei, Taiwan). For measurements performed at different temperatures, the heating rate was always below 0.2 °C/min.

Time-resolved fluorescence measurements with t-PnA were performed using $\lambda_{exc} = 295$ nm (using a secondary laser of Rhodamine 6 G) and $\lambda_{em} = 405$ nm. The experimental decays were analyzed using TRFA software (Scientific Software Technologies Center, Minsk, Belarus). For a decay described by a sum of exponentials, where α_i is the normalized pre-exponential and τ_i is the lifetime of the decay component i, the mean fluorescence lifetime is given by $<\tau> = \sum_i \alpha_i \tau_i^2 / \sum_i \alpha_i \tau_i$.

2.3. Confocal fluorescence microscopy and fluorescence correlation spectroscopy (FCS)

POPC/ceramide giant unilamelar vesicles (GUV) were prepared by electroformation [16]. Confocal fluorescence microscopy was performed using a Leica TCS SP5 (Leica Mycrosystems CMS GmbH, Mannheim, Germany) inverted microscope (DMI6000) with a 63× water (1.2 numerical aperture) apochromatic objective. Rho-DOPE (probe/lipid ratio 1/500) excitation was achieved using the 514 nm line from the Ar^+ laser. The emission was collected from 550 to 680 nm.

FCS measurements were performed using the same optical path described for the fluorescence imaging, with the exception that the fluorescence signal from the sample was detected by the avalanche photodiodes (APD) in the FCS unit, rather than the PMT (photomultiplier). A filter-cube containing a dichroic filter was used to separate the emitted light into two different detection channels and band pass filters 470–500 and 535–585 were used for spectral selection. GUVs labeled with Rho-DOPE (probe/lipid ratio 1/50,000–1/100,000) were used in different experiments and only the top side of the GUV was evaluated. Before starting the measurements, the Z-plane with higher intensity was selected. Six to ten successive autocorrelation curves were obtained for a single GUV and recorded during 20 s per FCS measurement. The average correlation curves were normalized for a better comparison between vesicles with different lipid composition. Autocorrelation curves were fitted using a two-dimensional Gaussian model in the absence of a triplet state [23]. To estimate the radius of the detection area ω_0 on the focal plane (calibration of the apparatus), the three-dimensional diffusion coefficient of Rho 110 freely diffusing in water was measured. A new calibration was performed on each day of the experiments.

3. Results

3.1. Impact of ceramide acyl-chain structure on gel domain formation

We previously demonstrated that t-PnA fluorescence lifetime and anisotropy are suitable parameters to characterize ceramide-induced alterations in simple [8,16] and complex [13,24] model membranes.

The presence of ceramide-enriched gel domains leads to a strong increase in both fluorescence lifetime and anisotropy of t-PnA towards characteristic values of its incorporation in a very rigid medium [8]. In the current study, we use this probe to explore the effect of ceramide-acyl chain structure on the properties of a fluid membrane. Five different ceramide species were selected as representative of those found in cellular membranes: long-chain (C16- and C18-) versus very long chain (C24-), and saturated (C16-, C18-, C24-) versus monounsaturated (C18:1- and C24:1-). Fig. 2 shows the fluorescence anisotropy of t-PnA for the different mixtures at room and physiological temperatures (24 °C and 37 °C). At room temperature (Fig. 2A), saturated ceramides display similar behavior independent of their chain length, whereas at physiological temperature (Fig. 2B) very small differences are observed, particularly for C18-ceramide. The sharp increase in t-PnA anisotropy confirms the strong ability of these ceramides to segregate into gel domains (at both temperatures) [8] even at a very low molar fraction. At very high ceramide molar fractions (above 80 mol%), saturated ceramides form a highly ordered gel phase that exclude t-PnA, which is translated by a decrease in t-PnA fluorescence anisotropy (data not shown), as previously described for C16-ceramide [8]. The combined effect of unsaturation/acyl chain length is shown in Fig. 2C and D. Similar to other unsaturated lipids [25], the presence of an unsaturated chain significantly decreases the ability of ceramide to drive gel-fluid phase separation compared to their saturated counterparts. This is clearly observed from the lower t-PnA fluorescence anisotropy in POPC/unsaturated ceramide mixtures, especially in the low-to-medium ceramide molar fraction range (Fig. 2C and D). Interestingly, the differences in the anisotropy trend of variation for the unsaturated ceramide species indicate that, despite the strong asymmetry of the very long chain C24:1-ceramide, its ability to induce the formation of a gel phase is higher compared to C18:1-ceramide. Furthermore, at physiological temperature, C18:1-ceramide is unable to drive gel-fluid phase separation, as shown by the constant and low anisotropy values, typical of a fluid phase [8]. t-PnA fluorescence lifetime variation (Fig. S1) further confirms the conclusions obtained from anisotropy data for all the POPC/ceramide mixtures.

To further explore the effect of the different ceramides on the fluid membrane, t-PnA fluorescence anisotropy was measured as a function of temperature. In these studies a transition between the gel and fluid phase can be detected by a strong and sharp decrease of the anisotropy values. As already described for some ceramide species [8,16], increasing the ceramide molar fraction shifts the main transition temperature of the mixtures towards higher values, independently of the ceramide structure (Fig. S2). Fig. 3 shows the melting profile of mixtures containing different concentrations of saturated (A and B) or unsaturated (C and D) ceramides. From this figure (panel A) and from Fig. S2A–C, it is possible to conclude that the melting profile of ceramide gel domains is dependent on the acyl chain length for concentrations up to 30 mol% of saturated ceramide. For instance, the melting temperature increases ~7 °C in mixtures containing 10 mol% ceramide, as the chain length is increased from C18- to C24- (Fig. S2). Interestingly, low amounts of C16-ceramide have a stronger impact on the melting profile of the mixtures as compared to C18-ceramide (Fig. 3), suggesting that C16-ceramide gel domains might be bigger (which is supported by microscopy studies, see Fig. 6) and/or could be more stable than those formed by C18-ceramide. This could be explained by the increase in ceramide acyl chain length giving rise to an increase in the average area per molecule [18]. At higher ceramide molar fractions (≥40 mol %), the effect of the acyl chain length is less pronounced, suggesting that the global properties of the membranes are similar (Fig. 3B). For the mixtures containing unsaturated ceramide species (Figs. 3C and D and S2D and E), the anisotropy profile of variation is dependent on the acyl chain length, with the main transition temperature shifted towards higher values at all the concentrations studied. Moreover, the melting of C18:1-ceramide-enriched gel domains always occurs at temperatures below the physiological temperature (Fig. S2 D).

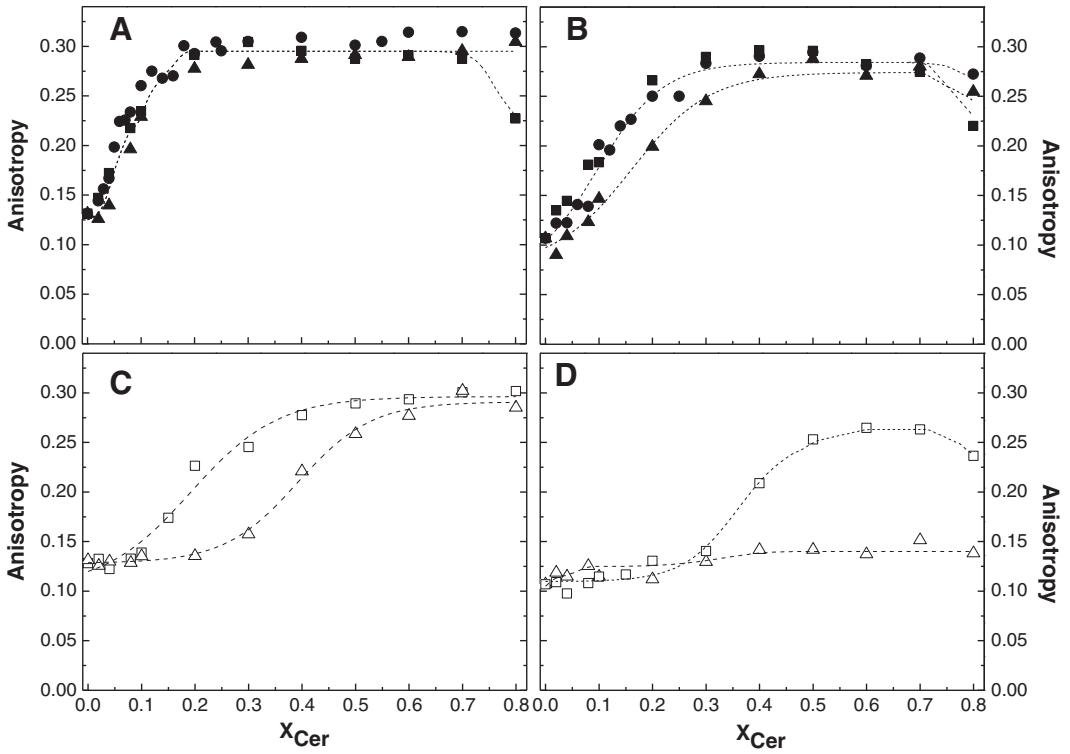

Fig. 2. Fluorescence anisotropy of t-PnA in (A, B) saturated and (C, D) unsaturated POPC/ceramide mixtures at (A, C) 24 °C and (B, D) 37 °C. (●) POPC/C16-ceramide, (▲) POPC/C18-ceramide, (■) POPC/C24-ceramide, (Δ) POPC/C18:1-ceramide and (□) POPC/C24:1-ceramide. Values correspond to an average (SD ≤ 0.015) of at least 3 independent experiments.

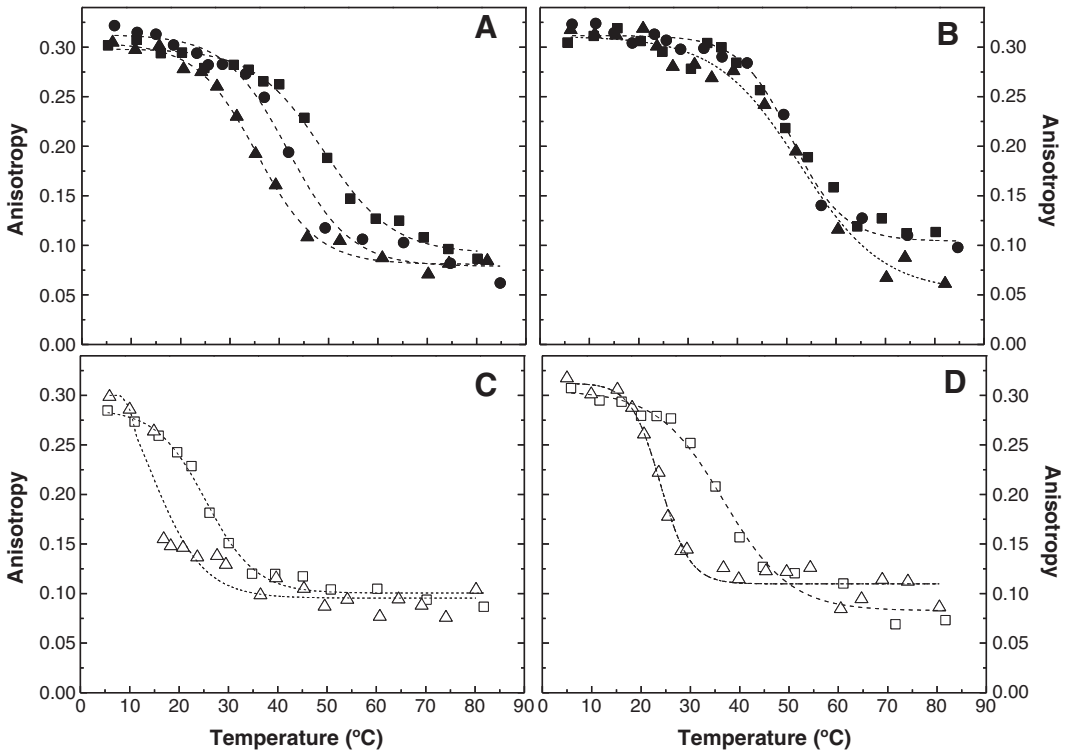

Fig. 3. Steady-state fluorescence anisotropy of t-PnA as a function of temperature in MLVs composed of (A, B) saturated and (C, D) unsaturated POPC/ceramide mixtures containing (A, C) 20 and (B, D) 40 mol% ceramide. (●) POPC/C16-ceramide, (▲) POPC/C18-ceramide, (■) POPC/C24-ceramide, (△) POPC/C18:1-ceramide and (□) POPC/C24:1-ceramide. Values are the average (SD < 0.015) of at least 3 independent experiments.

From the anisotropy variation as a function of temperature, it is possible to determine the *liquidus* boundaries of the binary POPC/ceramide phase diagrams [8]. Fig. 4 shows the *liquidus* boundaries determined in this study, as well as the partial phase diagrams previously determined for POPC/C16-ceramide (Fig. 4A) and POPC/C24:1-ceramide (Fig. 4B) [8,16]. As mentioned earlier, the phase behavior of POPC/saturated ceramide mixtures is similar and only small differences are detected for mixtures containing C18-ceramide (Fig. 4A). The miscibility of saturated ceramides in the fluid phase is low, i.e., ceramide is able to form gel domains even at low concentrations. In contrast, unsaturated ceramides present higher miscibility in the fluid phase and the *liquidus* boundary is placed at lower temperatures, particularly for C18:1-ceramide (Fig. 4B).

3.2. Characteristics of ceramide-enriched gel phase domains

We previously demonstrated that C16-ceramide segregates into highly ordered gel domains able to exclude fluorescent probes that commonly partition into gel domains, such as DPH [8]. On the other hand, this probe can partially partition into the less packed C24:1-ceramide gel domains [16]. To further investigate the characteristics of the domains formed in the different POPC/ceramide mixtures, DPH

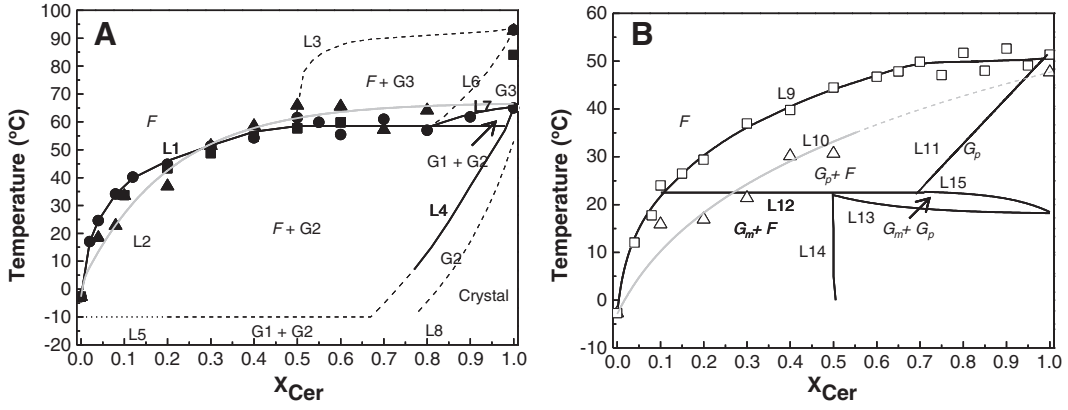

Fig. 4. POPC/ceramide partial binary phase diagram. The full lines are experimentally determined. (A) *liquidus* boundaries determined in this study for POPC/C18-ceramide (L2, ▲) and POPC/C24-ceramide (L1, ■) mixtures. The *liquidus* boundary of POPC/C16-ceramide overlays POPC/C24-ceramide *liquidus* boundary (L1, ■). For comparison, POPC/C16-ceramide binary phase diagram is also shown [8]. In this diagram, the dashed lines are the best estimates based on thermodynamic rules, photophysical parameters of the probes and transmission electron microscopy micrographs (see [8] for further details). (B) *Liquidus* boundaries of POPC/C18:1-ceramide (L10,△) and POPC/C24:1-ceramide (L9, □) mixtures. For comparison, POPC/C24:1-ceramide binary phase diagram is also shown (see [16] for further details). Abbreviations correspond to: F — fluid phase, G1 — POPC rich gel phase, G2 — ceramide rich gel phase; G3 — highly ordered ceramide rich gel phase, Gm, mixed interdigitated gel phase; Gp, partially interdigitated gel phase.

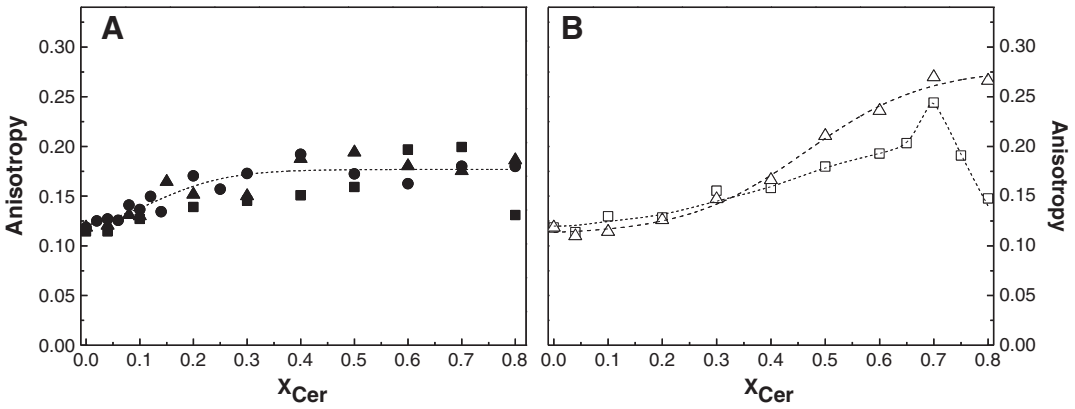

Fig. 5. Steady-state fluorescence anisotropy of DPH at 24 °C in (A) saturated and (B) unsaturated POPC/ceramide mixtures. (●) POPC/C16-ceramide, (▲) POPC/C18-ceramide, (■) POPC/C24-ceramide, (Δ) POPC/C18:1-ceramide and (□) POPC/C24:1-ceramide. Values are the average (SD < 0.01) of at least 3 independent experiments.

anisotropy was measured (Fig. 5). In mixtures with saturated ceramides, DPH anisotropy increases only to a small extent, demonstrating that the probe is excluded from the gel domains formed by these ceramides (Fig. 5A). In contrast, DPH anisotropy increases with ceramide content in mixtures containing unsaturated ceramides, showing the ability of the probe to incorporate into the gel phase to a certain extent (Fig. 5B). These results confirm that the gel phase formed by the unsaturated ceramides is less compact than the one formed by saturated ceramide.

From the anisotropy variation as a function of ceramide content (Fig. 5B), it is possible to determine the partition coefficient of DPH between a gel phase enriched in C18:1-ceramide and a fluid phase enriched in POPC ($K_p^{g/f}$), as described in ([26], Eq. 4). Our results indicate that DPH distributes equally between gel and fluid phase ($K_p^{g/f} = 1.00 \pm 0.11$) in POPC/C18:1-ceramide mixtures, suggesting that the properties of C18:1-ceramide gel phase are similar to the gel phase formed by other lipids, such as SM [27] and DPPC (1,2-dipalmitoyl-*sn*-glycero-3-phosphocholine) [28], and distinct from the other ceramide species.

To obtain information regarding the extent of phase separation, morphology and characteristics of the domains formed by each ceramide, confocal fluorescence microscopy was performed on GUVs.

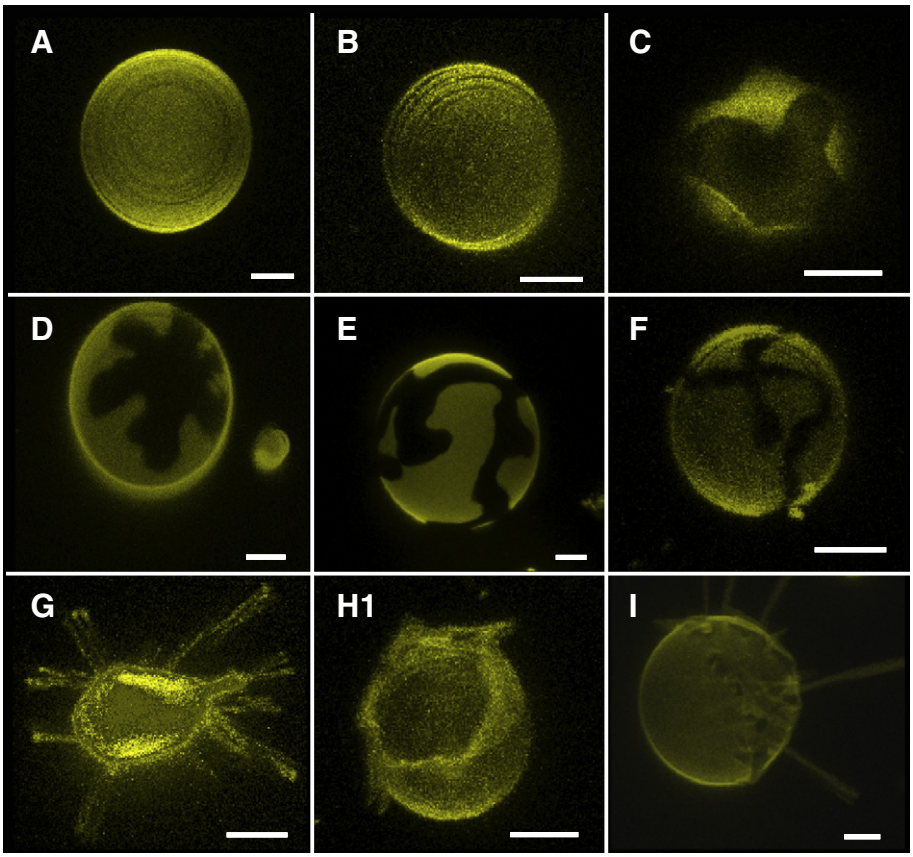

Fig. 6. Confocal fluorescence microscopy of POPC/ceramide mixtures. 3D projection images are obtained from 0.4 μm confocal slices of GUVs labeled with Rho-DOPE. The GUVs contain (A) POPC and POPC with 30 mol% of (B) C18:1-ceramide, (C) C24:1-ceramide, (D) C16-ceramide, (E) C18-ceramide and (F) C24-ceramide. Tubular structures were observed for (G) 70:30 POPC/C24:1-ceramide, (H) 70:30 POPC/C24-ceramide and (I) 70:15:15 POPC/C16-ceramide/C24:1-ceramide mixtures. Scale bars correspond to 5 μm.

Fig. 6 shows representative images of different POPC/ceramide mixtures. Distinct features are observed among the different mixtures such as i) increasing the length of the acyl chain of saturated ceramides leads to a decrease in the size of gel domains (dark areas), in agreement with previous observations in monolayers [18]; ii) the homogeneous labeling of POPC/C18:1-ceramide mixtures (Fig. 6B) indicates that no gel-fluid phase separation occurs for the concentration range studied, in agreement with spectroscopy data (Figs. 2C and S1 and S2); iii) the contrast between dark and bright areas in the POPC/saturated ceramide mixtures (Fig. 6D-F) is higher than for POPC/C24:1-ceramide (Fig. 6C) showing that Rho-DOPE is totally excluded from the former mixtures, while it can be partially incorporated into C24:1-ceramide enriched gel domains. This further corroborates DPH anisotropy data, showing the lower packing ability of unsaturated ceramide; iv) the morphologies of the domains are different among different ceramides, with C16-ceramide and C24:1-ceramide segregating into 'flower-like' shape domains, whereas the domains formed by C18- and C24-ceramide are elongated with round-shaped areas; v) very long chain ceramides are able to promote the formation of tubular structures independent of the degree of unsaturation (Fig. 6G and H). The formation of such tubules is likely to arise from the ability of very long chain ceramides to interdigitate, as previously shown for C24:1-ceramide [16]. To further test the hypothesis that interdigitation and or asymmetry (between C24-ceramide or C24:1-ceramide and POPC) are determinants in tubule formation, we performed a control experiment where 70 mol% POPC/15 mol% C24:1-ceramide/15 mol% C16-ceramide mixture (Fig. 6I) was used. The resultant mixture presented tubules which were not seen either in mixtures containing C16-ceramide (Fig. 6C) or mixtures containing less than 20 mol% C24:1-ceramide (16) (mixtures not able to form gel phase). These results suggest that the presence of C16-ceramide enhances the ability of C24:1-ceramide to form gel phase, and thus interdigitated phases, with consequent alteration of the local shape of the membrane.

3.3. Effect of ceramide-gel domains on the fluid phase

It is known that the formation of C16-ceramide gel domains drives an increase in the order of the fluid phase [8,29]. This can be observed by the variation in DPH anisotropy with ceramide content (Fig. 5A): the probe is excluded from the gel phase and the slight anisotropy increase is due to an increase in the packing of POPC acyl chains. An identical pattern was observed for mixtures containing C18- and C24-ceramides.

To further explore this effect, FCS was performed. Rho-DOPE was used to monitor the changes in the fluid phase. Fig. 7A shows the autocorrelation curves of Rho-DOPE in pure POPC and POPC with 30 mol% C16-ceramide. In the presence of ceramide, there is a shift in the autocorrelation curve that corresponds to a slower diffusion coefficient of the probe in the fluid phase, as further shown in Fig. 7B, where the diffusion coefficient, *D*, is plotted as a function of ceramide molar fraction for C16-, C18- and C24:1-ceramide- containing mixtures. Increasing the amount of the saturated ceramides (up to 30 mol%) leads to a decrease in *D*, until a plateau is reached, showing that the fluid phase becomes more ordered. Note that, this trend of variation is similar to that observed for DPH anisotropy (Fig. 5A), suggesting that increasing the amount of the gel phase has no further impact on the properties of the fluid phase. The diffusion coefficient of Rho-DOPE in POPC/C24:1-ceramide mixtures presents a different behavior; there is an initial increase in *D* compared to pure POPC, suggesting that the presence of C24:1-ceramide promotes a looser packing of the fluid phase. Further increasing the content of C24:1-ceramide above 20 mol% drives a decrease in *D* and thus, an increase in the packing of the fluid phase. It should be stressed that at room temperature and below 20 mol%, C24:1-ceramide is not able to segregate into gel domains when mixed with POPC (Figs. 2C and S1B and S2E) [16]. Therefore, the initial decrease in the order of the fluid phase is likely to be not only due to unsaturation but also due to the strong asymmetry of this lipid. Our previous studies with POPC/C24:1-ceramide mixtures showed that this ceramide is able to form interdigitated gel phases [16]. In the fluid phase, the looser packing of the acyl chains might facilitate the adjustment of the longer acyl chain of ceramide, minimizing the need for interdigitation, and likely introducing looser packing. Increasing C24:1-ceramide levels above 20 mol% leads to the formation of gel domains with a consequent impact on the order of the fluid phase, although to a smaller extent compared to the saturated species.

4. Discussion

Ceramide is a minor component of the plasma membrane, but in response to intra- and extracellular stimuli, its levels can be significantly increased [2]. Ceramide acts on several cellular processes such as apoptosis, inflammation, cell proliferation, and others [3]. It is likely that these processes are related to ceramide structure, composition and concentration [9,14] and mediated by ceramide-induced alterations on membrane biophysical properties [4]. Ceramide is one of the most hydrophobic lipids found in mammalian cells and has a strong tendency to segregate into ceramide-enriched gel domains or platforms [2,8]. In this study we evaluate the effect of biologically relevant ceramides (C16-C24) both on the physical and in the structural properties of a fluid membrane, with particular relevance on the impact of the chain length and degree of unsaturation of ceramide species.

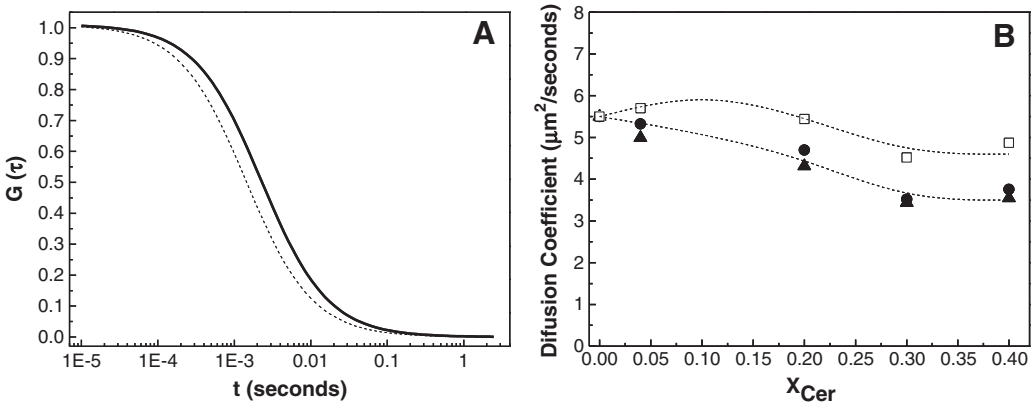

Fig. 7. FCS of GUVs labeled with Rho-DOPE. (A) Autocorrelation curves for Rho-DOPE in POPC (dashed line) and 70:30 POPC/C16-ceramide (solid line) GUVs. (B) Rho-DOPE diffusion coefficient in GUVs containing 0-to-40 mol% of (●) C16-ceramide, (▲) C18-ceramide and (□) C24:1-ceramide. The measurements were made at 22 °C. Values are the average (SD < 0.3) of at least 3 independent experiments.

4.1. Impact of ceramide structure on the physical properties of a fluid membrane

Our results demonstrate that the effect of ceramide on membrane properties was very dependent on its structure. Saturated ceramides are poorly miscible in the fluid lipid, POPC, and thus low amounts are required to promote gel domain formation. Interestingly, only very small differences (mainly on the melting profile of the gel domains) were detected among different saturated ceramide species, showing that acyl chain length does not play a strong role on gel/fluid phase separation. This is further reflected by the similarity in the *liquidus* line of the partial binary phase diagrams. A similar behavior was previously reported for C18- and C24-galactosylceramide in fluid membranes [30]. It was shown by ^{2}H NMR that C24-galactosylceramide was not more prone to segregate laterally than C18- species, and that the similarity in the order parameter profiles along most of the chain indicated that the basic fit of the galactosylceramide within the fluid matrix is the same regardless of the chain length. However, introduction of unsaturation markedly increased glycosphingolipid miscibility [17,31]. The same effect was observed in the present study: introduction of a double bond in the ceramide structure increased its miscibility and decreased its ability to form gel domains.

In contrast to that observed for saturated ceramides, the chain length of the unsaturated ceramides strongly affected their ability to promote gel-fluid phase separation, in particular, C18:1-ceramide is unable to segregate into gel domains at physiological temperature.

Interestingly, the properties of the gel domains formed by unsaturated and saturated ceramides are distinct. Unsaturated ceramides segregate into gel domains with characteristics similar to other lipids (e.g. SM), while saturated ceramides form highly ordered gel domains, showing that generation of saturated ceramides in the plasma membrane might have a stronger impact on its biophysical properties. Additionally, it was shown that the presence of ceramide gel domains promote an increase in the packing of POPC acyl chains. This could be attributed to the effect of a minor ceramide concentration in the fluid phase (~2 mol%) [8]. However, upon increasing the saturated ceramide molar fraction (Fig. 7B), there is a concomitant decrease in the Rho-DOPE diffusion coefficient, i.e. the fluid phase becomes more rigid. According to the lever rule, for a given temperature, the composition of the phases is constant, and only the fraction of each phase changes. In this way, the amount of saturated ceramide in the fluid is always close to 2 mol% [8]. Therefore, the increased order in the fluid must be due to a long range effect of the ceramide-enriched gel domains.

4.2. Membrane-induced structural alterations are dependent on ceramide structure

Although the global physical properties of membranes were similar in mixtures containing saturated ceramide species, remarkable structural differences were observed for these mixtures. First, the size of the domains and the amount of gel phase decreases with increasing saturated ceramide chain length. A similar observation was made by Karttunen et al. [18] in monolayers containing 1,2-dimeryristoyl-*sn*-glycero-3-phosphocholine (DMPC) and different acyl chain ceramides. The authors showed that the membrane becomes more condensed in the presence of C16-ceramide, as a result of a minimum in hydrophobic mismatch and increased van der Waals interactions, while increasing the acyl chain length promotes an increase in the repulsive potential between ceramide molecules and thus, a higher miscibility in the fluid. However, these studies were performed in monolayers and the repulsive potential arises from the longer chain that protrudes above the monolayer, which is not the case in our bilayer systems. Additionally, our results suggest that the miscibility of saturated ceramides in POPC is comparable because of the similarity between the *liquidus* lines in the partial phase diagrams (Fig. 4A).

Alternatively, an increased entrapment of fluid POPC within the C16-ceramide gel phase domains, compared to the other saturated ceramides, would explain the differences observed in the size of the domains. Small patches of fluid areas can be present within the gel domains and not observable because are below the resolution of the microscope. Interestingly, the differences in the morphology of the domains formed by C16-ceramide and the other two saturated ceramides support this explanation. According to Karttunen et al. [18], irregular or flower-like shape domains can be a consequence of a diffusion-limited phase transformation where domain growth proceeds through expulsion of the fluid molecules. On the other hand, if nucleation was the driving force, the interface instabilities would be lower and the domains would be rounder. Several parameters affect domain grow and morphology [18,32,33]. Normally, domains grow through the propagation of a so-called stable phase (typically solid) through a metastable phase (fluid), creating an unstable interface that forms patterns because of the competition between factors that stabilize the interface, namely line tension, and those that destabilize, such as, chemical potential, electrostatic repulsions, van der Waals interactions, etc. A stable interface is obtained when line tension is minimized, usually when round domains are formed. Instabilities of the interface are therefore due to the dominant effect of the destabilizing factors.

Besides the differences observed in the shape and size of the domains, strong morphological alterations, such as tubules, were also identified for mixtures containing very long chain ceramides (C24- and C24:1-). This process is likely to be mediated by interdigitation, as previously shown for POPC/C24:1-ceramide mixtures [16]. The interdigitation is related to the strong asymmetry of the molecules where the penetration of the longer acyl chain into the opposite leaflet facilitates the accommodation of the molecule in the bilayer and minimizes packing constraints [34]. There are several reports showing the ability of different lipids to form interdigitated phases [34–36] and/or tubular structures [37]. Yager et al. [38] showed, by low angle X-ray scattering and freeze fracture electron microscopy, that 1,2-bis(l,l2-tricosadiynoyl)-sn-glycero-3-phosphocholine ($DC_{23}PC$) formed tubules in water where the acyl chains of the lipid were tilted and partially interdigitated. Interdigitation and molecular tilting will increase headgroup spacing, which may produce significant differences in molecular packing in fluid and solid phases. The system may tend to minimize headgroup spacing differences by inducing membrane bending and thus, promoting tubule formation.

5. Conclusions

In this study, we demonstrate that differences in ceramide acyl chain structure lead to distinct alterations in the properties of a fluid membrane. The most remarkable differences are detected between membranes containing saturated- versus unsaturated-ceramides, although the acyl chain length also has a strong impact on membrane properties, especially when considering unsaturated ceramides. This might be of particular significance when considering differences in the distribution of the CerS among various tissues [39] and thus the distribution of ceramides with defined chain lengths; the different biophysical properties of each ceramide may be of importance in explaining different signaling pathways that are activated in specific tissues and cells. Recently, for instance, we have shown that a mouse lacking CerS2 has strong physiological and pathological alterations in the liver [40,41], but the global membrane properties only change to a small extent, likely due to a compensation mechanism that changes the SL composition in such a way that membrane fluidity is maintained. Membrane enrichment in a particular ceramide may also drive morphological alterations through the formation of tubular structures, which have a strong impact on cell function, namely at the

level of cell-to-cell communication and lipid sorting and trafficking [42,43].

The fact that only small differences are detected among different acyl chain saturated ceramides may suggest the existence of a fine-tuning mechanism of ceramide-dependent biological processes that, from a biophysical point of view, may depend more strongly on the interface properties of the domains than on global changes in the physical properties of the membranes.

Acknowledgements

The authors thank Alexander Fedorov for assistance with time-resolved fluorescence measurements. A.H. Futerman is The Joseph Meyerhoff Professor of Biochemistry at the Weizmann Institute of Science. This work was supported by Fundação para a Ciência e Tecnologia (FCT), Portugal (PTDC/QUI-BIQ/111411/2009) and Israel Science Foundation grant number 1735/07. FCT provided a research grant to S.N.P. (SFRH/BD/46296/2008).

Appendix A. Supplementary data

Supplementary data to this article can be found online at doi:10.1016/j.bbamem.2011.07.023.

References

[1] G. van Meer, J.C.M. Holthuis, Sphingolipid transport in eukaryotic cells, Biochim. Biophys. Acta 1486 (2000) 145–170.
[2] H. Grassmé, J. Riethmuller, E. Gulbins, Biological aspects of ceramide-enriched membrane domains, Prog. Lipid Res. 46 (2007) 161–170.
[3] Y.A. Hannun, L.M. Obeid, Principles of bioactive lipid signalling: lessons from sphingolipids, Nat. Rev. Mol. Cell Biol. 9 (2008) 139–150.
[4] F.M. Goñi, F.X. Contreras, L.R. Montes, J. Sot, A. Alonso, Biophysics (and sociology) of ceramides, Biochem. Soc. Symp. (2005) 177–188.
[5] Y. Pewzner-Jung, S. Ben Dor, A.H. Futerman, When do lasses (longevity assurance genes) become CerS (ceramide synthases)? Insights into the regulation of ceramide synthesis, J. Biol. Chem. 281 (2006) 25001–25005.
[6] N. Bartke, Y.A. Hannun, Bioactive sphingolipids: metabolism and function, J. Lipid Res. 50 (2009) S91–S96.
[7] B. Westerlund, P.M. Grandell, Y. Isaksson, J. Slotte, Ceramide acyl chain length markedly influences miscibility with palmitoyl sphingomyelin in bilayer membranes, Eur. Biophys. J. 39 (2010) 1117–1128.
[8] L. Silva, R.F.M. De Almeida, A. Fedorov, A.P.A. Matos, M. Prieto, Ceramide-platform formation and -induced biophysical changes in a fluid phospholipid membrane, Mol. Membr. Biol. 23 (2006) 137–150.
[9] J. Sot, F.J. Arand, M.I. Collado, F.M. Goñi, A. Alonso, Different effects of long- and short-chain ceramides on the gel-fluid and lamellar-hexagonal transitions of phospholipids: a calorimetric, NMR, and X-ray diffraction study, Biophys. J. 88 (2005) 3368–3380.
[10] M.L. Fanani, B. Maggio, Kinetic steps for the hydrolysis of sphingomyelin by Bacillus cereus sphingomyelinase in lipid monolayers, J. Lipid Res. 41 (2000) 1832–1840.
[11] M.L. Fanani, S. Hartel, B. Maggio, L. De Tullio, J. Jara, F. Olmos, R.G. Oliveira, The action of sphingomyelinase in lipid monolayers as revealed by microscopic image analysis, Biochim. Biophys. Acta 1798 (2010) 1309–1323.
[12] Ira, L.J. Johnston, Sphingomyelinase generation of ceramide promotes clustering of nanoscale domains in supported bilayer membranes, Biochim. Biophys. Acta 1778 (2008) 185–197.
[13] L.C. Silva, A.H. Futerman, M. Prieto, Lipid raft composition modulates sphingomyelinase activity and ceramide-induced membrane physical alterations, Biophys. J. 96 (2009) 3210–3222.
[14] J.M. Holopainen, J. Lemmich, F. Richter, O.G. Mouritsen, G. Rapp, P.K.J. Kinnunen, Dimyristoylphosphatidylcholine/C16:0-ceramide binary liposomes studied by differential scanning calorimetry and wide- and small-angle X-ray scattering, Biophys. J. 78 (2000) 2459–2469.
[15] F.M. Goñi, A. Alonso, Effects of ceramide and other simple sphingolipids on membrane lateral structure, Biochim. Biophys. Acta 1788 (2009) 169–177.
[16] S.N. Pinto, L.C. Silva, R.F.M. de Almeida, M. Prieto, Membrane domain formation, interdigitation, and morphological alterations induced by the very long chain asymmetric C24:1 ceramide, Biophys. J. 95 (2008) 2867–2879.
[17] J.M. Holopainen, H.L. Brockman, R.E. Brown, P.K.J. Kinnunen, Interfacial interactions of ceramide with dimyristoylphosphatidylcholine: impact of the N-acyl chain, Biophys. J. 80 (2001) 765–775.
[18] M. Karttunen, M.P. Haataja, M. Säily, I. Vattulainen, J.M. Holopainen, Lipid domain morphologies in phosphatidylcholine–ceramide monolayers, Langmuir 25 (2009) 4595–4600.
[19] D.C. Carrer, S. Schreier, M. Patrito, B. Maggio, Effects of a short-chain ceramide on bilayer domain formation, thickness, and chain mobililty: DMPC and asymmetric ceramide mixtures, Biophys. J. 90 (2006) 2394–2403.
[20] D.C. Carrer, E. Kummer, G. Chwastek, S. Chiantia, P. Schwille, Asymmetry determines the effects of natural ceramides on model membranes, Soft Matter 5 (2009) 3279–3286.
[21] M.P. Veiga, J.L. Arrondo, F.M. Goñi, A. Alonso, Ceramides in phospholipid membranes: effects on bilayer stability and transition to nonlamellar phases, Biophys. J. 76 (1999) 342–350.
[22] M. Fidorra, L. Duelund, C. Leidy, A.C. Simonsen, L.A. Bagatolli, Absence of fluid-ordered/fluid-disordered phase coexistence in ceramide/POPC mixtures containing cholesterol, Biophys. J. 90 (2006) 4437–4451.
[23] N. Kahya, D. Scherfeld, K. Bacia, B. Poolman, P. Schwille, Probing lipid mobility of raft-exhibiting model membranes by fluorescence correlation spectroscopy, J. Biol. Chem. 278 (2003) 28109–28115.
[24] B.M. Castro, R.F.M. de Almeida, L.C. Silva, A. Fedorov, M. Prieto, Formation of ceramide/sphingomyelin gel domains in the presence of an unsaturated phospholipid: a quantitative multiprobe approach, Biophys. J. 93 (2007) 1639–1650.
[25] F. Separovic, K. Gawrisch, Effect of unsaturation on the chain order of phosphatidylcholines in a dioleoylphosphatidylethanolamine matrix, Biophys. J. 71 (1996) 274–282.
[26] L.C. Silva, R.F.M. de Almeida, B.M. Castro, A. Fedorov, M. Prieto, Ceramide-domain formation and collapse in lipid rafts: membrane reorganization by an apoptotic lipid, Biophys. J. 92 (2007) 502–516.
[27] R.F.M. de Almeida, A. Fedorov, M. Prieto, Sphingomyelin/phosphatidylcholine/cholesterol phase diagram: boundaries and composition of lipid rafts, Biophys. J. 85 (2003) 2406–2416.
[28] L.F. Aguilar, C.P. Sotomayor, E.A. Lissi, Main phase transition depression by incorporation of alkanols in DPPC vesicles in the gel state: influence of the solute topology, Colloids Surf. 108 (1996) 287–293.
[29] Y.W. Hsueh, R. Giles, N. Kitson, J. Thewalt, The effect of ceramide on phosphatidylcholine membranes: a deuterium NMR study, Biophys. J. 82 (2002) 3089–3095.
[30] D. Lu, D. Singh, M.R. Morrow, C.W.M. Grant, Effect of glycosphingolipid fatty acid chain length on behavior in unsaturated phosphatidylcholine bilayers: a deuterium NMR study, Biochemistry 32 (1993) 290–297.
[31] S. Ali, H.L. Brockman, R.E. Brown, Structural determinants of miscibility in surface films of galactosylceramide and phosphatidylcholine: effect of unsaturation in the galactosylceramide acyl chain, Biochemistry 30 (1991) 11198–11205.
[32] A. Gutierrez-Campos, G. Diaz-Leines, R. Castillo, Domain growth, pattern formation, and morphology transitions in langmuir monolayers. A new growth instability, J. Phys. Chem. B 114 (2010) 5034–5046.
[33] A. Flores, E. Corvera-Poiré, C. Garza, R. Castillo, Pattern formation and morphology evolution in Langmuir monolayers, J. Phys. Chem. B 110 (2006) 4824–4835.
[34] T.J. Mcintosh, S.A. Simon, J.C. Ellington, N.A. Porter, New structural model for mixed-chain phosphatidylcholine bilayers, Biochemistry 23 (1984) 4038–4044.
[35] C. Huang, Mixed-chain phospholipids and interdigitated bilayer systems, J. Mol. Med. 68 (1990) 149–165.
[36] C.h. Huang, J.T. Mason, Structure and properties of mixed-chain phospholipid assemblies, Biochim. Biophys. Acta 864 (1986) 423–470.
[37] A.S. Goldstein, A.N. Lukyanov, P.A. Carlson, Y. Paul, M.H. Gelb, Formation of high-axial-ratio-microstructures from natural and synthetic sphingolipids, Chem. Phys. Lipids 88 (1997) 21–36.
[38] P. Yager, R.R. Price, J.M. Schnur, P.E. Schoen, A. Singh, D.G. Rhodes, The mechanism of formation of lipid tubules from liposomes, Chem. Phys. Lipids 46 (1988) 171–179.
[39] E.L. Laviad, L. Albee, I. Pankova-Kholmyansky, S. Epstein, H. Park, A.H. Merrill, A.H. Futerman, Characterization of ceramide synthase 2: tissue distribution, substrate specificity, and inhibition by sphingosine 1-phosphate, J. Biol. Chem. 283 (2008) 5677–5684.
[40] Y. Pewzner-Jung, O. Brenner, S. Braun, E.L. Laviad, S. Ben Dor, E. Feldmesser, S. Horn-Saban, D. Amann-Zalcenstein, C. Raanan, T. Berkutzki, R. Erez-Roman, O. Ben David, M. Levy, D. Holzman, H. Park, A. Nyska, A.H. Merrill, A.H. Futerman, A critical role for ceramide synthase 2 in liver homeostasis, J. Biol. Chem. 285 (2010) 10911–10923.
[41] Y. Pewzner-Jung, H. Park, E.L. Laviad, L.C. Silva, S. Lahiri, J. Stiban, R. Erez-Roman, B. Brugger, T. Sachsenheimer, F. Wieland, M. Prieto, A.H. Merrill, A.H. Futerman, A critical role for ceramide synthase 2 in liver homeostasis, J. Biol. Chem. 285 (2010) 10902–10910.
[42] A. Rustom, R. Saffrich, I. Markovic, P. Walther, H.H. Gerdes, Nanotubular highways for intercellular organelle transport, Science 303 (2004) 1007–1010.
[43] B. Sorre, A. Callan-Jones, J.B. Manneville, P. Nassoy, J.F. Joanny, J. Prost, B. Goud, P. Bassereau, Curvature-driven lipid sorting needs proximity to a demixing point and is aided by proteins, Proc. Natl. Acad. Sci. U. S. A. 106 (2009) 5622–5626.